

Damped DQE model updating of a three-story frame using experimental data

Laleh Fatahi^{a, *}, Shapour Moradi and Ali Hajnayeb

^a Mechanical Engineering Department, Shahid Chamran University of Ahvaz, Ahvaz, Iran

ARTICLE INFO

Article history:

Received: 02 September 2020

Accepted: 09 September 2020

Keywords:

Differential Quadrature Element Method

Evolutionary Optimization Algorithms

Damped Model Updating

Mechanical Vibrations

Frames

ABSTRACT

In this paper, following a two-stage methodology, the differential quadrature element (DQE) model of a three-story frame structure is updated for the vibration analysis. In the first stage, the mass and stiffness matrices are updated using the experimental natural frequencies. Then, having the updated mass and stiffness matrices, the structural damping matrix is updated to minimize the error between the experimental and numerical damping ratios. Note that two different damping models are used, including a diagonal matrix with unknown diagonal elements and a general damping model. Since the structural joints of the frames are not completely rigid in practice, several parameters are used to model the flexibility of these joints. The optimum values of the material and geometrical design parameters are obtained by updating the DQE model using the experimental modal parameters obtained through modal testing. Considering the robustness of the evolutionary optimization algorithms in the model updating practice, a combination of particle swarm optimization and artificial bee colony algorithm, that benefits from the advantages of both approaches, is utilized. By updating the DQE model, the effectiveness of the evolutionary optimization algorithms, especially in a high-dimensional optimization problem, e.g., finding the optimum general damping matrix, is studied. The results show that, considering the geometrical lengths of the frame as the design parameters, the natural frequencies of the updated model match better with the experimental ones. In addition, using the general damping matrix, the errors of the damping ratios significantly are decreased.

1. Introduction

The differential quadrature element method (DQEM) introduced by Chen [1], is a robust and computationally efficient numerical method that utilizes the DQ rule [2] to discretize the differential equations, continuity, and boundary conditions governing each element in the numerical model of structures. The application of the DQ method has been successfully investigated in a variety of engineering problems [3-12]. Since there are always some uncertainties in physical and elemental parameters of the numerical models of structures, different model updating schemes are utilized to estimate the uncertain parameters based on experimentally obtained data. These methods can be classified as direct and iterative ones or in another classification as gradient-based methods and non-gradient ones with random computations. A good review of different updating methods was done by Mottershead and Friswell [13]. While all the updating methods are aimed to reduce the difference between the outputs of the

numerical model and those of the real structure, each has its own pros and cons. The direct methods are computationally efficient and are therefore proper for large, complicated models; however, the updated matrices may not be physically correct. Among the iterative methods, selection of the design parameters can help to estimate uncertainties in the model, but the convergence of the gradient-based approaches depends highly on the initial guess for the design parameters. On the contrary, the success of the random iterative algorithms does not depend on the initial model, which is, in fact, selected randomly from the search space, but the drawback of these methods is their computational costs where the best result is usually obtained after lots of iterations. Since proper selection of the design parameters plays an important role in the success of all the updating procedures, a sensitivity analysis is usually performed, and the design parameters to which the output of the model is insensitive are avoided. Different techniques for sensitivity analysis can be utilized to estimate local and global sensitivities of the model output to the design parameters. A

* Corresponding author. lfatahi@scu.ac.ir

review of the available techniques for parameter sensitivity analysis was presented by Hamby [14]. When a global representation of structures, e.g., a frame structure, is of interest, it is unnecessary and computationally expensive to have a model with many details. In such cases, one-dimensional elements are commonly used; however, one of the facing challenges is how to model the joints efficiently. Since the welded joints are not completely rigid in practice, one way to deal with flexibility of the joint is using rotational and/or translational springs, but it is not an efficient model mainly because the modal parameters of the structure are almost insensitive to the associated stiffness parameters of the springs [15]. In the following work, to model the flexibility of the welded joints in a frame structure, the effective lengths of the members connected by the joints are increased and the effect of using these geometrical design parameters on the accuracy of the updated model is also studied. The optimum values of these parameters in a specific range are obtained by solving an optimization problem. The objective is to minimize the sum of the squared differences between the numerical and experimental modal parameters of the structure. Considering the robustness of the evolutionary algorithms, the particle swarm inspired multi-elitist artificial bee colony (PS-MEABC) algorithm [16] which benefits from the advantages of both the particle swarm optimization (PSO) method [17] and the artificial bee colony (ABC) algorithm [18], is used to solve the problem. In most literatures dealing with model updating of structures, the damping characteristics of the structures are neglected. However, without damping identification, the vibration amplitude at resonance frequencies cannot be predicted. Even if there is no viscous damping, the inherent structural damping still exists and affects the response of the structures. Therefore, to have a more accurate numerical model, the structural damping matrix of the model should also be included in the updating procedure. Maia et al. [19] discussed the need to develop the identification methodologies of general damping models and addressed the difficulties facing researchers. Adhikari [20] developed fundamental methods for the analysis and identification of a general non-viscous damping model. Arora et al. [21] updated the damped finite element model of an F-shape structure using the experimental FRF data by focusing on the joints' parameters. They modeled the joints using vertical and torsional springs and updated the mass and stiffness matrices using an iterative sensitivity-based method while the damping matrix was updated using a direct method. The maximum error in their prediction of the natural frequencies in the updated model was 3.6% which could be even better if the joints were modeled more efficiently. Arora [22] also proposed a direct method to identify the structural damping matrix using a complete normal FRF matrix.

In the suggested two-stage updating procedure of the DQE model, using the experimental modal parameters of a damaged three-story frame and utilizing an iterative random evolutionary algorithm e.g., the PS-MEABC algorithm, the DQE model of the frame is updated. In the first stage of the updating, to update the mass and stiffness matrices, Young's modulus, density, and some geometrical and elemental design parameters to recover the flexibility of the joints, are considered as design parameters. To verify the suggested design parameters, local and global sensitivities of the natural frequencies to the design parameters are evaluated. By choosing different sets of design parameters, it is shown how the selection of the design parameters will affect the accuracy of the results. Besides, for damping identification, two different structural damping models are used. In the first one, the damping matrix is assumed to be diagonal, while in the second model, a general damping model is used and all the elements of

the damping matrix are identified. The robustness and simplicity of the evolutionary algorithms, especially in the case of a problem with high dimensions, e.g., identifying all the elements of the damping matrix, make them a good candidate for engineering optimization problems. Their drawback of being computationally expensive can also be tackled by high-performance computers.

2. The differential quadrature element model of the frame

In the case of a uniform cross-section and constant Young's modulus, and following the Euler-Bernoulli beam theory, the differential equations governing the axial and transverse vibrations of a frame element (see Figure (1)) are stated by Eqs. (1-2).

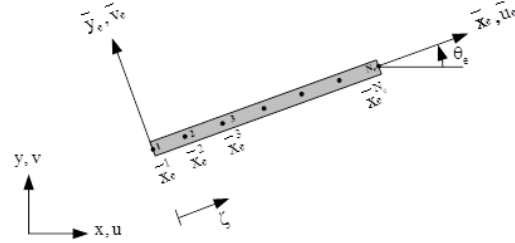


Figure 1. One-dimensional differential quadrature frame element

$$E_e A_e \frac{d^2 \bar{u}_e^i}{dx_e^2} + \rho_e A_e \omega^2 \bar{u}_e^i = 0 \quad (1)$$

$$i = 2, 3, \dots, N_e - 1$$

$$E_e I_e \frac{d^4 \bar{v}_e^i}{dx_e^4} - \rho_e A_e \omega^2 \bar{v}_e^i = 0 \quad (2)$$

$$i = 3, 4, \dots, N_e - 2$$

where \bar{u}_e^i and \bar{v}_e^i are the i th node's axial and transverse displacements in the local coordinate system of e th element, ω is the natural frequency, E_e , A_e , ρ_e , I_e and N_e stands for Young's modulus, the area of the cross-section, the density, the area moment of inertia and the number of nodes of the e th element, respectively. Moreover, using the DQ rule, the n th derivation of the function f can be evaluated as the weighted summations of the function values at the domain nodes.

$$\left. \frac{\partial^n f}{\partial x^n} \right|_{x=x_i} = \sum_{j=1}^{N_e} C_{ij}^{(n)} f_j \quad (3)$$

where $C^{(n)}$ is the weighting matrix of the n th derivative. Employing the DQ rule on Eqs. (1) and (2), one can obtain Eq. (4).

$$\left(\frac{E_e I_e}{l_e^4} C_v^{(4)} - \rho_e A_e \omega^2 \mathbf{I}_v \right) \bar{\delta}_e = 0 \quad (4)$$

$$\left(\frac{E_e A_e}{l_e^2} C_u^{(2)} + \rho_e A_e \omega^2 \mathbf{I}_u \right) \bar{\delta}_e = 0 \quad (5)$$

in which l_e and $\bar{\delta}_e$ are the length and the displacement vector of the e th element, $C_u^{(i)}$ and $C_v^{(i)}$ are the weighting coefficient matrices of the i th order derivative of u and v , respectively. \mathbf{I}_u and \mathbf{I}_v are identity matrices [23]. Eqs. (3) and (4) can be expressed in the following matrix form.

$$(\bar{\mathbf{k}}_e - \omega^2 \bar{\mathbf{m}}_e) \bar{\delta}_e = 0 \quad (6)$$

where $\bar{\mathbf{k}}_e$ and $\bar{\mathbf{m}}_e$ are the stiffness and mass matrices of the e th element. Considering a frame structure with M_e elements, the governing equations of the vibrations of the system can be stated by Eq. (7).

$$(\mathbf{K} - \omega^2 \mathbf{M}) \delta = 0 \tag{7}$$

where

$$\delta = [\delta_1 \ \delta_2 \ \dots \ \delta_{M_e}]^T \tag{8}$$

$$\delta_i = \left\{ u_i^1 \ v_i^1 \ u_i^{-2} \ v_i^{-2} \ \dots \ u_i^{-N_e-1} \ v_i^{-N_e-1} \ u_i^{N_e} \ v_i^{N_e} \right\} \tag{9}$$

$$\mathbf{M} = \begin{bmatrix} \mathbf{m}_1 & & & \\ & \mathbf{m}_2 & & \\ & & \ddots & \\ & & & \mathbf{m}_{M_e} \end{bmatrix}_{2M_e(N_e-3), 2M_e N_e} \tag{10}$$

$$\mathbf{K} = \begin{bmatrix} \mathbf{k}_1 & & & \\ & \mathbf{k}_2 & & \\ & & \ddots & \\ & & & \mathbf{k}_{M_e} \end{bmatrix}_{2M_e(N_e-3), 2M_e N_e} \tag{11}$$

To take into account the damping effects, Eq. (7) is modified by adding the structural damping matrix \mathbf{D} as follows.

$$(\mathbf{K} + j \mathbf{D} - \omega^2 \mathbf{M}) \delta = 0 \tag{12}$$

Note that by employing the boundary and continuity conditions, one can relate the displacements of the boundary points to those of the domain points and define Eq. (12) only in terms of the domain points. Detailed descriptions regarding the DQEM applied to frame structures can be found in an article written by Fatahi and Moradi [23]. Considering the fact that many damaged engineering structures are still at work, and proper modeling of them is of great importance, a three-story cracked frame is chosen as the experimental case study. Assuming the crack only affects its vicinity, Rizos et al. [24] analyzed a cracked beam as two segments that were connected by a rotational spring; the spring constant K_θ was found using Eq. (13). This method is utilized in the current work to model the cracks.

$$K_\theta = \frac{EI}{6(1-\nu^2)h} \frac{1}{f(\alpha/b)} \tag{13}$$

where EI , ν , h , and a are the bending stiffness, the Poisson's ratio, the height of the beam, and the crack depth, respectively. $f(\alpha/b)$ is also a modification factor defined in Eq. (14).

$$f\left(\frac{\alpha}{b}\right) = 1.8224\left(\frac{\alpha}{b}\right)^2 - 3.95\left(\frac{\alpha}{b}\right)^3 + 16.375\left(\frac{\alpha}{b}\right)^4 - 37.226\left(\frac{\alpha}{b}\right)^5 + 76.81\left(\frac{\alpha}{b}\right)^6 - 126.9\left(\frac{\alpha}{b}\right)^7 + 172\left(\frac{\alpha}{b}\right)^8 - 143\left(\frac{\alpha}{b}\right)^9 + 66.56\left(\frac{\alpha}{b}\right)^{10} \tag{14}$$

3. Experimental model of the damaged three-story steel frame

To construct a small scale three-story steel frame, two column and three beam members were welded together as shown in Figure (2). To give a nearly clamped condition to the ends, the columns were welded to a thick beam which was itself bolted to a heavy basement. All the welded beads of the joints were then grinded to remove the excess metal. Besides, to have a damaged structure, two cracks were artificially introduced in the structure using a coping saw. The normalized depths of the cracks on the left and right columns are 0.5 and 0.3, respectively. To obtain the experimental model of the structure, modal testing was performed to extract the experimental modal parameters. The equipment used to perform a roving hammer modal test is listed in Table (1).

Table 1. The equipment used for modal testing of the cracked frame structure

Equipment	Description
Impact Hammer	AU02 with plastic tip - Global Test
Accelerometer	Magnet-mounted Piezoelectric Accelerometer A/120/V DJB
Data Acquisition System and Signal Analyzer	6/1-ch Input/Output Module Type 3032A B&K with Pulse LabShop Software

Each point of the total of 82 points shown in Figure (3) was hit by the hammer twice. Note that the impact locations were selected based on a combination of Optimum Driving Point¹ and Average Driving DOF Velocity² techniques [25]. The ODP technique is used to find DOFs that are close to or at nodal lines of the modes in the frequency range of interest. For a DOF located near the nodal line of a specific mode, the value of the modal constant of that mode is close to zero. Therefore, to identify whether a DOF is close to the nodal lines of the m modes, all modal constants of that DOF for all selected modes should be multiplied as mentioned in Eq. (15). Those DOFs with non-zero ODP values can be chosen as possible impact locations.

¹ ODP

² ADDOFV

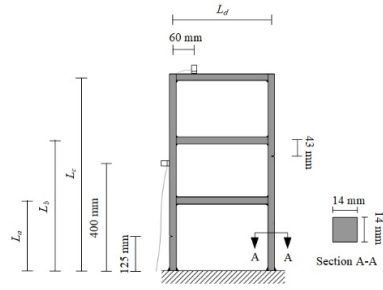


Figure 2. The experimental setup of the three-story frame on the left, the geometrical properties on the right

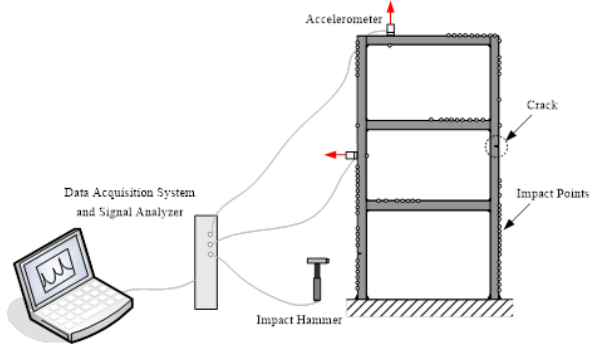


Figure 3. Schematic of the roving hammer modal test performing on the three-story frame structure

$$ODP(i) = \prod_{r=1}^m \|\phi_{i,r}\| \quad (15)$$

Besides, to reduce the risk of double-hits while impacting the structure, one should avoid hitting the points with high average velocity. The ADDOFV parameter defined in Eq. (16) is then used to find the average velocity of each DOF.

$$ADDOFV(i) = \sum_{r=1}^m \frac{\phi_{i,r}^2}{\omega_r} \quad (16)$$

Combining both *ODP* and *ADDOFV* techniques, the DOFs with higher values of *ODP/ADDOFV* are the best ones to be impacted. In addition, to select the best locations to measure the response of the structure, *ADDOFA-EI*¹ method is used [25]. This method is based on the effective independence technique [26] modified by the *ADDOFA* parameter (see Eq. (17)). The main goal is to have a full rank experimental mode shape matrix whose elements do not as well have low responses.

$$ADDOFA(i) = \sum_{r=1}^m \phi_{i,r}^2 \quad (17)$$

By performing the modal test, the FRFs² were evaluated using PULSE LabShop software in the frequency range of 0-800 Hz with a frequency increment of 0.125 Hz. Figure (4) illustrates one of the experimentally obtained FRF diagrams. The experimental FRFs were then exported to the MScope software where the multi-reference complex mode indicator function³ and the multi

reference polynomial methods were utilized to extract the experimental modal parameters. Note that an exponential time window with a time constant of 2 seconds was applied to the captured time responses, which increased the apparent damping of the measured FRFs. Thus, the added damping was removed from the extracted damping ratios.

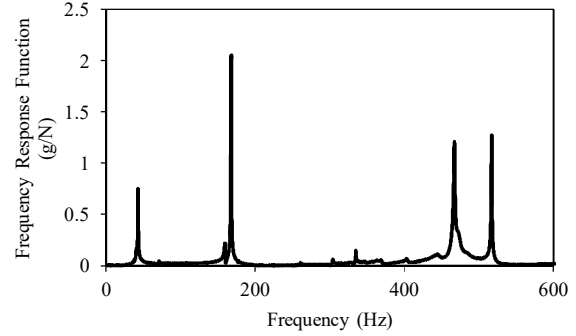


Figure 4. An experimentally obtained FRF diagram

4. The DQE Model updating using the PS-MEABC algorithm

To update the DQE model of the frame using the experimental data, an optimization problem is defined in which the objective function is constructed using the weighted summation of the squared error between the natural frequencies of the experimental and the DQE models, as stated in Eq. (18).

$$F = \sum_{i=1}^{N_m} w_i \left(\frac{\omega_i^e - \omega_i^d}{\omega_i^e} \right)^2 \quad (18)$$

where w_i is the weighting factor of the i th mode used to represent the confidence in the measurement and N_m is the number of modes. The subscripts e and d also refer to the experimental and DQE models, respectively. Considering equal measurement accuracy for all the N_m modes, all the weighting factors are assumed to be unity. As seen in Eq. (18), only the natural frequencies are used in the updating process and the measured mode shape data are only utilized to assure the correspondence between the experimental and numerical modes. Therefore, they are not used in the construction of the objective function. This is mainly because the experimental natural frequencies are obtained easily even from a single or a few FRF diagrams, while extraction of proper mode shapes of real-life structures usually requires lots of FRF measurements as well as accessibility to all parts of the structure, which is not always possible. Therefore, for the sake of applicability, the objective function only consists of the natural frequencies. After defining the objective function, the PS-MEABC algorithm is utilized to minimize Eq. (18) based on the experimental data obtained from modal testing. The next two sections are devoted to the discussion on the methodology of the PS-MEABC algorithm and the selection of the design parameters.

¹ Average Driving DOF Acceleration - Effective Independence

² Frequency Response Functions

³ CMIF

4.1. The particle swarm inspired multi-elitist artificial bee colony algorithm

The artificial bee colony (ABC) algorithm was first introduced by Karaboga [18] and since then has been applied to solve many engineering problems [27-28]. The ABC algorithm imitates the social behavior of honey bees in finding and exploiting food sources to construct an optimization method. The swarm in the ABC algorithm consists of employed bees, onlookers and scouts. Using the explorations and exploitations, the bees can find the best food source, or in the optimization terminology, the best solution. Unlike the gradient-based optimization approaches, the convergence of the ABC algorithm does not depend on the initial guess of the design parameters; however, it has some drawbacks in the exploitation phase. Xiang et al. [14] modified the standard ABC algorithm and developed a particle swarm inspired multi-elitist artificial bee colony algorithm that improves the exploitation in the ABC by inspiration from the PSO algorithm. The PS-MEABC algorithm is described in Figure (5) in which Eqs. (19) to (23) are utilized. To initialize N random solutions, Eq. (19) is used for i from 1 to N .

$$X_{ij} = LB_j + \theta(UB_j - LB_j) \tag{19}$$

where X_{ij} is the j th parameter of the i th solution, LB_j and UB_j are the lower and upper bounds of the parameter j , respectively, and θ is a random number between 0 and 1. The updating equation for the employed bees is mentioned in Eq. (20).

$$X_{updated\ ij} = X_{ij} + V_{ij} \tag{20}$$

The modification factor V_{ij} is defined by Eq. (21).

$$V_{ij} = X_{ij} + \beta_{ij}(X_{ij} - X_{kj}) + \alpha_{ij}(X_{ij} - EL_{Sel_i,j}) \tag{21}$$

where k is the index of a randomly selected solution, and β and α are the two random matrices whose elements are between -1 and 1. $EL_{Sel_i,d}$ stands for the value of d th dimension of the elitist chosen by the roulette wheel method, and Sel_i is the selected index. The probability of the i th solution is also calculated by Eq. (22).

$$P_i = \frac{fitness(i)}{\sum_{i=1}^N fitness(i)} \tag{22}$$

To find a neighborhood food source for an onlooker bee, Eq. (23) is utilized.

$$V_{ij} = X_{ij} + \beta_{ij}(X_{ij} - X_{kj}) + \alpha_{ij}(X_{ij} - gbest_j) \tag{23}$$

where $gbest_j$ is the j th dimension of the best global solution found so far. Moreover, based on the boundary treatment in the standard ABC algorithm, if one dimension of the solution goes beyond its boundary, then its value is set to the boundary value in both the employed and onlooker bees phases. In the PS-MEABC algorithm, for the onlooker bee phase, the boundary treatment is similar to the standard ABC, but in the employed bees phase, the value of the parameter exceeding the boundary is set to that of the selected elitist, i.e. if $X_{ij} > UB_j$ or $X_{ij} < LB_j$, then $X_{ij} = EL_{Sel_i,j}$ to keep the population diverse [14].

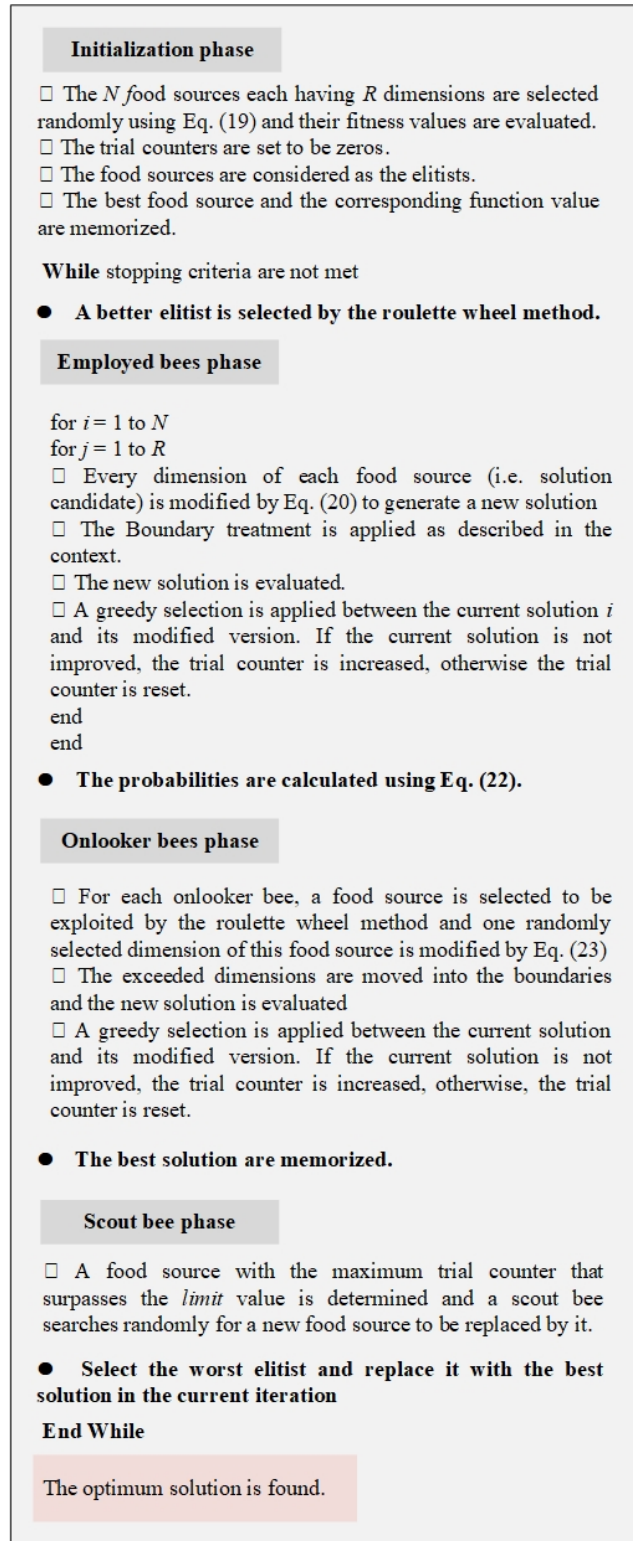


Figure 5. The main steps of the PS-MEABC algorithm [14]

5. Results and Discussions

Modeling the structures especially with one-dimensional elements imposes some geometrical simplifications to the numerical models. Therefore, these models always have some uncertainties due to the way that the boundary conditions or joints are defined, and also due to the material properties of the

structures. To estimate these uncertainties, different updating methods can be utilized where the selection of proper design parameters is very crucial. The output of the model (e.g., the natural frequencies) should be sensitive to the selected design parameters; otherwise, the updating procedure fails to achieve an accurate model. To find the most influential design parameters on the output of the model, sensitivity analysis can be performed. From one point of view, methods of sensitivity analysis can be classified into local and global analyses. A local analysis examines the sensitivity relative to a specific estimate of the parameter value while a global analysis investigates the sensitivity with regard to the entire domain of the parameter. The design parameters having high global sensitivity can speed up the exploration phase of the evolutionary optimization algorithms while the high local sensitivity to the design parameter can improve the exploitation phase. Note that a high global sensitivity to a parameter does not imply its high local sensitivity and vice versa. Therefore, to improve the efficiency of both exploration and exploitations phases, and thereby to speed up the convergence of the updating (i.e. optimization) method, the global and local sensitivities of the model output to the suggested design parameters should be investigated separately.

5.1. Sensitivity Analysis

One of the simplest local sensitivity analyses is one-at-a-time¹ method [30], in which one input parameter is changed by a percentage of its baseline value while other parameters are held constant. The sensitivity index is then determined by calculating the ratio of the change in the output to the input parameter variation. A Similar procedure is repeated for each input parameter. Therefore, assuming X_i and Y as the i th input and the corresponding output of the model, respectively, the local sensitivity index is calculated using Eq. (24).

$$LSI_i = \frac{\Delta Y}{\Delta X_i} \frac{X_i}{Y} \tag{24}$$

where the multiplier X_i/Y is introduced to remove the effects of the units. A more powerful OAT method examines the variation in the output as each parameter is individually changed by a factor of its standard deviation. Thereby, the parameter's variability and the associated influence on the output of the model are also included [29].

In the structural optimizations, some of the most uncertain parameters belong to the welded joints. To take into account the flexibility of a welded joint, one of the methods is to replace the joint by a spring with uncertain stiffness parameter. This research aims at a more efficient modeling of the flexibility of welded joints. Thus, instead of using point springs and elastic foundations, the focus is on the bending and axial stiffness of the elements connected to the joint. In addition, modeling the structure with one-dimensional elements, the effective length of the members connected to the joint can also be increased to recover the joint flexibility. Therefore, to assess the effectiveness of the suggested joints' parameters, Young's modulus and the cross-sectional area of the elements connected by the joints, the geometrical lengths of

the beam and column members as shown in Figure (2), and two rotational springs to model the end supports are selected as the design parameters. To investigate the local and global sensitivities of the natural frequencies to the design parameters, a base-case DQE model of the frame is required. Table (2) provides the lower and upper bounds of each suggested design parameter. An average value of each parameter is utilized to construct a base-case DQE model.

Table 2. The suggested design parameters for the DQE model updating of the three-story steel frame

No.	Description	Symbol (Unit)	Lower Bound	Upper Bound
1	Density	ρ (Kg/m ³)	7700	7850
2	Young's modulus	E (N/m ²)	180e9	210e9
3	Geometrical length	L_d (m)	0.300	0.320
4	Geometrical length	L_a (m)	0.260	0.285
5	Geometrical length	L_b (m)	0.465	0.485
6	Geometrical length	L_c (m)	0.680	0.695
7-14	Young's modulus of the elements connected by the	E_1, E_2, \dots, E_8 (N/m ²)	140e9	220e9
15-22	Width of the cross-section of the elements connected by the	a_1, a_2, \dots, a_8 (m)	0.013	0.015
23-30	Height of the cross-section of the elements connected by the	b_1, b_2, \dots, b_8 (m)	0.013	0.015
31-32	Stiffness of the rotational springs at two ends	K_{t1}, K_{t2} (N.m/rad)	5e6	5e11

Note that the density and Young's modulus of the structure are included as the design parameters. The joint numbers are shown in Figure (6).

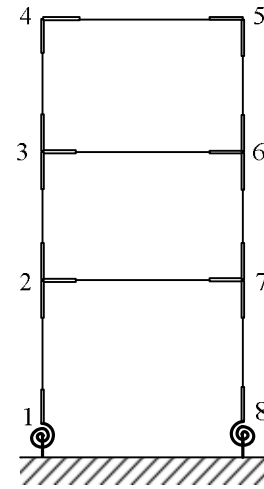


Figure 6. The joint numbers in the DQE model of the frame

The local sensitivity value of the natural frequencies to the design parameters is visualized in Figure (7). As observed in this figure, among the parameters utilized to model the joints, the highest local sensitivity values in all the first three modes are of the geometrical lengths L_c and the lowest ones are of the rotational springs used to model the flexibility of the support.

¹ OAT

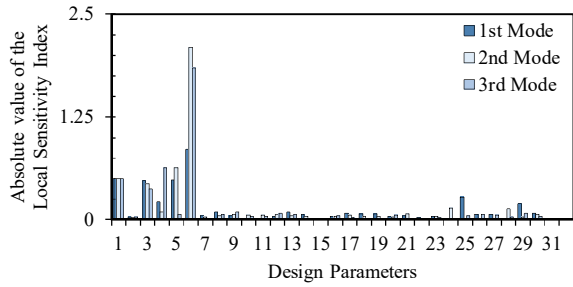


Figure 7. The local sensitivity indices of the natural frequencies to the design parameters

To quantify the global sensitivity, one can evaluate the variation in the output when changing one input parameter from its minimum to maximum values [30]. The global sensitivity index of the *i*th input parameter is then calculated as follows.

$$GSI_i = \frac{Y_{max} - Y_{min}}{Y_{max}} \quad (25)$$

where Y_{max} and Y_{min} are the outputs of the model using the maximum and minimum values of the *i*th input parameter, respectively. Figure (8) shows the GSI values of the first three natural frequencies to the suggested design parameters. The minimum GSI values are of the rotational springs which again confirm the low contributions of the springs' stiffness in the model updating procedure. The GSI of the other design parameters related to the joints, especially the geometrical lengths of the members and Young's modulus of the elements connected by joints, are good enough to approve their positive roles in the success of the model updating routine. Another method to investigate the global sensitivity of the model output to the input parameters is the employment of a simple random sampling method in the search space of each input parameter. In this work, 2000 random samples are selected from the uniform distribution of each design parameter in its domain while other parameters are kept fixed. Figure (9) illustrates the resulting change in the first natural frequency due to changes in $E, \rho, L_c, E_3, a_3, b_3, Kt_1$ and Kt_2 . As can be seen, while the relationship between E, ρ, L_c, E_3, a_3 and b_3 with the first natural frequency are almost linear, the changes introduced in the first natural frequency due to changing Kt_1 and Kt_2 are negligible. To better assess the relationship between the change in the natural frequencies and the change in the design parameters, the Spearman correlation coefficient can be utilized [31]. The Spearman coefficient is defined as the Pearson correlation coefficient between ranked variables. Considering x_i and y_i as the ranked variables corresponding to the X_i and Y_i , then the Spearman coefficient is given by Eq. (26).

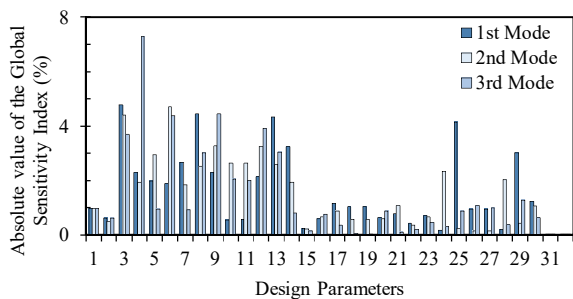


Figure 8. The global sensitivity indices of the natural frequencies to the design parameters

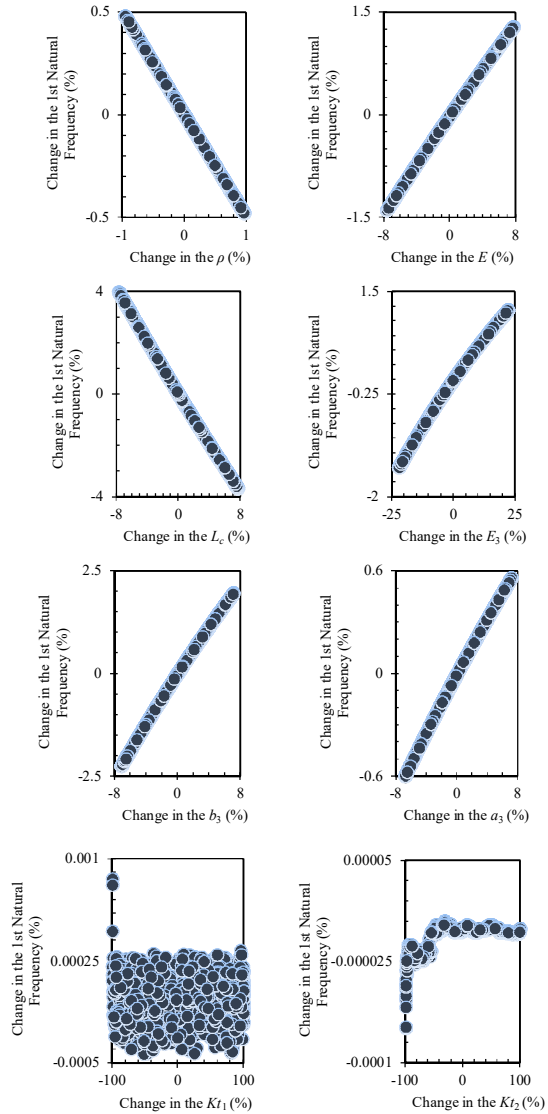


Figure 9. Percent change in the natural frequencies due to changing the design parameters for 2000 random samples

$$\rho = \frac{\sum_i (x_i - x_m)(y_i - y_m)}{\sqrt{\sum_i (x_i - x_m)^2 \sum_i (y_i - y_m)^2}} \quad (26)$$

Note that x_m and y_m are the average values of x and y , respectively. If Y tends to increase monotonically as X increases, the Spearman correlation coefficient will be +1. If Y tends to constantly decrease as X increases, the Spearman correlation coefficient gets the value of -1. A Spearman correlation of zero shows no tendency for Y to change as X changes. Figure (10) shows the evaluated Spearman correlation coefficients. The low values of this coefficient corresponding to the stiffness parameters of the springs prove the fewer tendencies of the natural frequencies to change as these stiffness parameters vary. The Spearman coefficients of other design parameters are close to +1 or -1 showing the monotonic relationships between the natural frequencies and these design parameters.

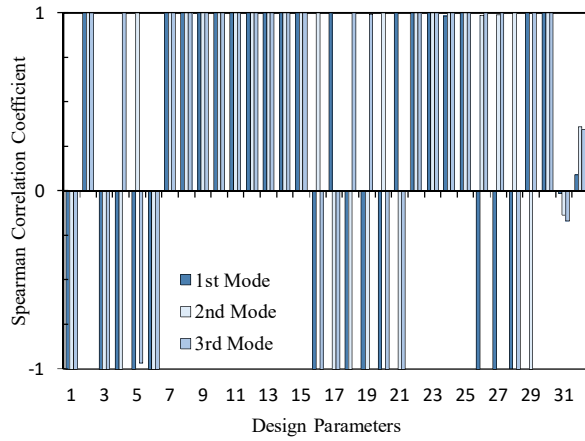


Figure 10. Spearman correlation coefficients between the natural frequencies and the design parameter

From the obtained results of the sensitivity analysis, one can conclude that in order to have an efficient random optimization algorithm, all the design parameters provided in Table (2) are acceptable except for Kt_1 and Kt_2 where in the selected search space, the value of local and global sensitivities of the natural frequencies to these two stiffness parameters were low.

5.2. Results of the DQE model updating

The updating process is performed in two stages. In the first stage, the mass and stiffness matrices are updated. To investigate how L_a, L_b, L_c and L_d (i.e. the geometrical design parameters) affect the accuracy of the updated model, two different sets of design parameters are utilized as described in Table (3). The swarm size of the PS-MEABC was set to 50 and after 25000 function evaluations, the optimum values of the design parameters have been recorded.

Table 3. Two different sets of design parameters

Design Parameter	Set 1	Set 2	Design Parameter	Set 1	Set 2
$E(N/m^2)$	✓	✓	$a_2(m)$	✓	✓
$\rho(Kg/m^3)$	✓	✓	$a_3(m)$	✓	✓
$L_a(m)$	×	✓	$a_4(m)$	✓	✓
$L_b(m)$	×	✓	$a_5(m)$	✓	✓
$L_c(m)$	×	✓	$a_6(m)$	✓	✓
$E_1(N/m^2)$	✓	✓	$a_7(m)$	✓	✓
$E_2(N/m^2)$	✓	✓	$a_8(m)$	✓	✓
$E_3(N/m^2)$	✓	✓	$b_1(m)$	✓	✓
$E_4(N/m^2)$	✓	✓	$b_2(m)$	✓	✓
$E_5(N/m^2)$	✓	✓	$b_3(m)$	✓	✓
$E_6(N/m^2)$	✓	✓	$b_4(m)$	✓	✓
$E_7(N/m^2)$	✓	✓	$b_5(m)$	✓	✓
$E_8(N/m^2)$	✓	✓	$b_6(m)$	✓	✓
$a_1(m)$	✓	✓	$b_7(m)$	✓	✓
			$b_8(m)$	✓	✓

The evolution of the best objective function value is illustrated in Figure (11), where a significantly lower objective value has been obtained using Set 2 of the design parameters. Table 4 contains the first five natural frequencies obtained from the experimental and the updated DQE models. It is seen that the frequency errors of Set 2 are considerably lower than those of Set 1. Hence, using optimum values of the Set 2 as tabulated in Table (5), more accurate results are obtained. The comparison of the mode shapes of the updated DQE model using Set 2 with the corresponding experimental ones is illustrated in Figure (12) which confirms the mode pairing of Table (4).

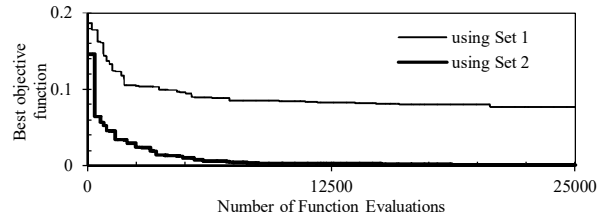


Figure 11. The evolution of the best objective function value

Table 4. The results obtained from the first stage of the model updating

Mode No.	Natural Frequency (Hz)		Absolute Relative Error (%)		
	EMA ¹	Updated DQE Model		Set 1	Set 2
		Set 1	Set 2		
1	42.500	43.770	42.503	2.988	0.007
2	167.625	167.644	167.701	0.011	0.045
3	334.500	319.605	334.448	4.453	0.015
4	467.250	466.934	467.222	0.068	0.006
5	517.250	518.098	517.256	0.164	0.001

Table 5. The optimum values of the design parameters (Set 2)

Design Parameter	Optimum Value	Design Parameter	Optimum Value
$E(N/m^2)$	209e9	$a_2(m)$	0.0135
$\rho(Kg/m^3)$	7743	$a_3(m)$	0.0146
$L_d(m)$	0.307	$a_4(m)$	0.0149
$L_a(m)$	0.284	$a_5(m)$	0.0132
$L_b(m)$	0.483	$a_6(m)$	0.0138
$L_c(m)$	0.685	$a_7(m)$	0.0134
$E_1(N/m^2)$	143e9	$a_8(m)$	0.0138
$E_2(N/m^2)$	165e9	$b_1(m)$	0.0138
$E_3(N/m^2)$	213e9	$b_2(m)$	0.0143
$E_4(N/m^2)$	212e9	$b_3(m)$	0.0136
$E_5(N/m^2)$	186e9	$b_4(m)$	0.0139
$E_6(N/m^2)$	186e9	$b_5(m)$	0.0141
$E_7(N/m^2)$	152e9	$b_6(m)$	0.0150
$E_8(N/m^2)$	140e9	$b_7(m)$	0.0131
$a_1(m)$	0.0144	$b_8(m)$	0.0139

¹ Experimental Modal Analysis

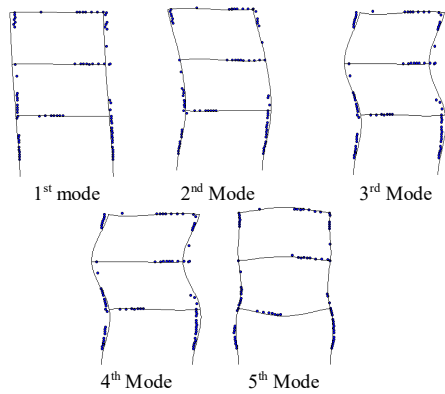
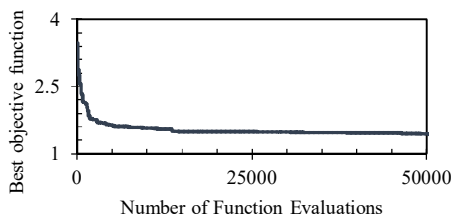
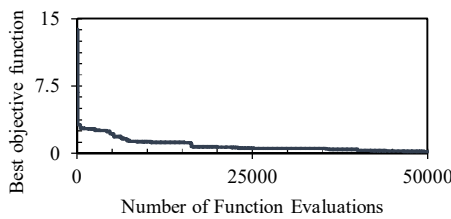


Figure 12. The first five mode shapes of the updated DQE model (solid lines) together with the corresponding experimental ones (solid circles)

In the next stage of the model updating procedure, the structural damping matrix is updated. Two different damping models are utilized; Model 1: a diagonal matrix with unknown diagonal elements and Model 2: a general damping model where all the elements of the damping matrix are unknown. The drawback of using a general damping model is having a large number of design parameters; however, utilizing an evolutionary optimization algorithm, e.g., the PS-MEABC algorithm, unlike the gradient-based approaches, no difficulty will arise in the convergence. As observed from Figure (13), after 50,000 function evaluations, Model 2 which utilizes a general damping model, has brought more accurate results. The damping ratios of the first five modes of the updated damped DQE models are compared with the experimental counterparts in Table (6). According to this table, using a general damping model, the 3rd and 4th modes have been improved significantly. The mesh of both diagonal and general damping matrices are shown in Figure (14).

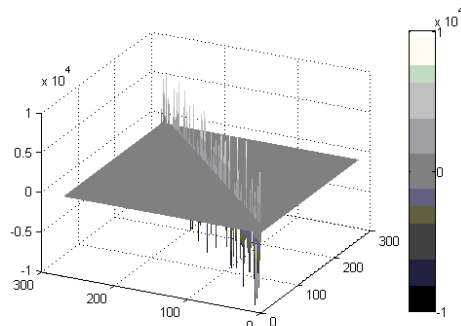


(a)

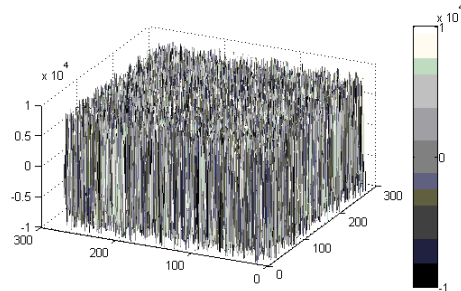


(b)

Figure 13. The evolution of the best objective function value during the optimization of (a) Model 1 (b) Model 2



(a)



(b)

Figure 14. The mesh of the damping matrix of (a) Model 1 (b) Model 2

Table 6. The results obtained from the second stage of the model updating

Mode No.	Damping Ratio (%)				Absolute Relative Error (%)	
	EMA	Updated Damped DQE		Model 1	Model 2	
		Model 1	Model 2			
1	0.262	0.261	0.260	0.038	0.076	
2	0.033	0.033	0.033	0.000	0.000	
3	0.120	0.021	0.116	82.500	3.333	
4	0.141	0.047	0.158	66.666	12.057	
5	0.039	0.039	0.039	0.000	0.000	

4. Conclusions

In this paper, a two-stage model updating scheme was utilized to update the differential quadrature element (DQE) model of frame structures. In the first stage, using an iterative random methodology, the mass and stiffness matrices were updated. The best design parameters, especially those related to the welded joints, were selected based on the local and global sensitivities of the natural frequencies to the candidate design parameters. The suggested updating procedure was applied to a three-story damaged frame structure. After evaluating different sensitivity indices, the density and Young's modulus of the structure, and several geometrical and elemental parameters related to the flexibility of the joints were selected as the design parameter. A modified artificial bee colony algorithm was then utilized to optimize the DQE model of the frame. It was observed that considering the geometrical lengths as the design parameters, decreased the errors in natural frequencies of the updated model. Furthermore, the damping matrix was also updated in the second stage of the model updating using two different structural damping models, diagonal and general damping matrices, where using the

second model brought a more accurate damped updated model, but it had a drawback of being computationally expensive. Nevertheless, the robustness and simplicity of the evolutionary algorithms, especially for a high-dimensional optimization problem, e.g., identifying all the elements of the general damping matrix, made them a good candidate for such engineering optimization problems. A High-performance computer could also alleviate the drawback of the computational costs.

References

- [1] C.N. Chen, The two-dimensional frame model of the differential quadrature element method, *Computers & Structures*, Vol. 62, No. 3, pp. 555-571, 1997.
- [2] R. Bellman, B. Kashef, J. Casti, Differential quadrature: a technique for the rapid solution of nonlinear partial differential equations, *Journal of Computational Physics*, Vol. 10, No. 1, pp. 40-52, 1972.
- [3] C.N. Chen, The DQEM analysis of vibration of frame structures having nonprismatic members considering warping torsion, *International Journal of Nonlinear Sciences and Numerical Simulation*, Vol. 2, No. 3, pp. 235-255, 2001.
- [4] C.N. Chen, DQEM analysis of out-of-plane vibration of nonprismatic curved beam structures considering the effect of shear deformation, *Advances in Engineering Software*, Vol. 39, No. 6, pp. 466-472, 2008.
- [5] M. Mohammadi, M. Ghayour, A. Farajpour, Analysis of free vibration sector plate based on elastic medium by using new version of differential quadrature method, *Journal of Simulation and Analysis of Novel Technologies in Mechanical Engineering*, Vol. 3, No. 2, pp. 47-56, 2010.
- [6] M. Danesh, A. Farajpour, M. Mohammadi, Axial vibration analysis of a tapered nanorod based on nonlocal elasticity theory and differential quadrature method, *Mechanics Research Communications*, Vol. 39, No. 1, pp. 23-27, 2012.
- [7] X. Wang, Y. Wang, Free vibration analysis of multiple-stepped beams by the differential quadrature element method, *Applied Mathematics and Computation*, Vol. 219, No. 11, pp. 5802-5810, 2013.
- [8] S. Asemi, A. Farajpour, H. Asemi, M. Mohammadi, Influence of initial stress on the vibration of double-piezoelectric-nanoplate systems with various boundary conditions using DQM, *Physica E: Low-dimensional Systems and Nanostructures*, Vol. 63, pp. 169-179, 2014.
- [9] M. Mohammadi, A. Farajpour, A. Moradi, M. Ghayour, Shear buckling of orthotropic rectangular graphene sheet embedded in an elastic medium in thermal environment, *Composites Part B: Engineering*, Vol. 56, pp. 629-637, 2014.
- [10] M. Safarabadi, M. Mohammadi, A. Farajpour, M. Goodarzi, Effect of surface energy on the vibration analysis of rotating nanobeam, *Journal of Solid Mechanics*, Vol. 7, No. 3, pp. 299-311, 2015.
- [11] M. Mohammadi, M. Safarabadi, A. Rastgoo, A. Farajpour, Hygro-mechanical vibration analysis of a rotating viscoelastic nanobeam embedded in a visco-Pasternak elastic medium and in a nonlinear thermal environment, *Acta Mechanica*, Vol. 227, No. 8, pp. 2207-2232, 2016.
- [12] A. Pouretamad, K. Torabi, H. Afshari, DQEM analysis of free transverse vibration of rotating non-uniform nanobeams in the presence of cracks based on the nonlocal Timoshenko beam theory, *SN Applied Sciences*, Vol. 1, No. 9, pp. 1092, 2019.
- [13] J. E. Mottershead, M. Friswell, Model updating in structural dynamics: a survey, *Journal of Sound and Vibration*, Vol. 167, No. 2, pp. 347-375, 1993.
- [14] D. M. Hamby, A review of techniques for parameter sensitivity analysis of environmental models, *Environmental Monitoring and Assessment*, Vol. 32, No. 2, pp. 135-154, 1994.
- [15] J. Mottershead, M. Friswell, G. Ng, J. Brandon, Geometric parameters for finite element model updating of joints and constraints, *Mechanical Systems and Signal Processing*, Vol. 10, No. 2, pp. 171-182, 1996.
- [16] Y. Xiang, Y. Peng, Y. Zhong, Z. Chen, X. Lu, X. Zhong, A particle swarm inspired multi-elitist artificial bee colony algorithm for real-parameter optimization, *Computational Optimization and Applications*, Vol. 57, No. 2, pp. 493-516, 2014.
- [17] J. Kennedy, R. Eberhart, Particle swarm optimization, in *Proceeding of the IEEE International Conference on Neural Networks*, 1995.
- [18] D. Karaboga, *An idea based on honey bee swarm for numerical optimization*, Technical report-tr06, Erciyes university, 2005.
- [19] N. Maia, J. Silva, A. Ribeiro, On a general model for damping, *Journal of Sound and Vibration*, Vol. 218, No. 5, pp. 749-767, 1998.
- [20] S. Adhikari, *Damping models for structural vibration*, PhD Thesis, University of Cambridge, 2000.
- [21] V. Arora, S. Singh, T. Kundra, On the use of damped updated FE model for dynamic design, *Mechanical Systems and Signal Processing*, Vol. 23, No. 3, pp. 580-587, 2009.
- [22] V. Arora, Structural damping identification method using normal FRFs, *International Journal of Solids and Structures*, Vol. 51, No. 1, pp. 133-143, 2014.
- [23] L. Fatahi, S. Moradi, Differential quadrature element model updating of frame structures, *Proceedings of the Institution of Mechanical Engineers, Part C: Journal of Mechanical Engineering Science*, Vol. 228, No. 7, pp. 1094-1107, 2014.
- [24] P. Rizos, N. Aspragathos, A. Dimarogonas, Identification of crack location and magnitude in a cantilever beam from the vibration modes, *Journal of Sound and Vibration*, Vol. 138, No. 3, pp. 381-388, 1990.
- [25] N. Imamovic, *Validation of large structural dynamics models using modal test data*, PhD Thesis, Department of Mechanical Engineering, Imperial College, 1998.
- [26] D. C. Kammer, Sensor placement for on-orbit modal identification and correlation of large space structures, *Journal of Guidance, Control, and Dynamics*, Vol. 14, No. 2, pp. 251-259, 1991.

- [27] S. Omkar, J. Senthilnath, R. Khandelwal, G. N. Naik, S. Gopalakrishnan, Artificial Bee Colony (ABC) for multi-objective design optimization of composite structures, *Applied Soft Computing*, Vol. 11, No. 1, pp. 489-499, 2011.
- [28] Z. Ding, R. Yao, J. Li, Z. Lu, Structural damage identification based on modified artificial bee colony algorithm using modal data, *Inverse Problems in Science and Engineering*, Vol. 26, No. 3, pp. 422-442, 2018.
- [29] D. J. Downing, R. Gardner, F. Hoffman, An examination of response-surface methodologies for uncertainty analysis in assessment models, *Technometrics*, Vol. 27, No. 2, pp. 151-163, 1985.
- [30] L. Bauer, D. Hamby, Relative sensitivities of existing and novel model parameters in atmospheric tritium dose estimates, *Radiation Protection Dosimetry*, Vol. 37, No. 4, pp. 253-260, 1991.
- [31] J. Myers, A. Well, *Research Design and Statistical Analysis* (2nd edn), Lawrence Erlbaum, 2003.